Shallow high-amplitude seismic anomalies characterization in the Hoop Fault Complex, Barents Sea

Satinder Chopra[+], Ritesh Kumar Sharma[+], Graziella Kirtland Grech[+], and Bent Erlend Kjølhamar[†]*

[+]Arcis Seismic Solutions, TGS, Calgary; [†]TGS, Asker, Norway

Summary

Shallow migrating hydrocarbon fluids in western Barents Sea are found to be associated with high seismic amplitudes, and focusing on the Hoop Fault Complex area therein, we have attempted to characterize such shallow high amplitude anomalies. The workflow followed for doing so entails the application of prestack simultaneous impedance inversion followed by analysis in Lambda-rho versus Mu-rho as well as P-impedance versus density crossplot space, and aims at discrimination of anomalies that are associated with the presence of hydrocarbons from those that are not. Finally, we suggest that such attempts be supplemented with the application of spectral decomposition as well as integration with diverse data types such as P-cable seismic as well as CSEM data, so as to come up with an integrated assessment for the prospects and mitigating risk.

Introduction

Many areas of the western Barents Sea host shallow as well as deep-seated hydrocarbon accumulations, wherefrom fluids are migrating to the sea floor (Bunz et al., 2014). Evidence of past episodes of gas migration can be seen in the form of pockmarks on the sea floor as well as vertical pipes or chimneys on seismic sections. Thus the detailed distribution of shallow migrating fluids or the presence of gas in the shallow zones in the areas under investigation is required, for which data with high vertical and spatial resolution is required.

We focus on the Hoop Fault Complex area in the western Barents Sea (Figure 1) and begin by exhibiting some of our observations of high amplitude anomalies on the shallow sections of the seismic data, whose characterization is our objective. Thereafter, we present the results of a workflow that was adopted for the discrimination of some of these high amplitude anomalies. This workflow entails the application of poststack impedance inversion, going on to prestack simultaneous impedance inversion and followed by the analysis of the results in Lambda-rho versus Mu-rho as well as P-impedance versus density crossplot space. Finally, we briefly mention the efforts being made in our industry for integration of seismic data with other types of data that are being acquired with state-of-the-art technology, all being aimed at mitigating exploration risk.

Based on the exploration work carried out so far, the Jurassic succession in the Hoop Fault Complex area has been the most successful. The Upper Jurassic Hekkingen Formation source rock is believed to be mature along the western and southern flanks of the basins adjacent to the Hoop Fault Complex. Of the five recently drilled wells in the area, Wisting Central and Hanssen proved oil in the Jurassic fault blocks between 500 to 800 m below the sea floor. Both these discoveries were supported by bright amplitude anomalies on the seismic. While the Apollo well came out dry, the Atlantis and Mercury wells, both resulted in small gas discoveries. The Mid- Triassic Kobbe, Upper Triassic Snadd and Mid-Jurassic Stø are the prospective formations of interest in this area.

Availability of seismic data and workflow adopted

A portion (500 km^2) of the 3D seismic volume covering over 22,000 km^2 in and around the Hoop Fault Complex was picked up for carrying out a feasibility analysis aimed at characterizing the bright seismic amplitude anomalies, and also examining the fault and channel features in detail. A straightforward choice for accomplishing this was to put the data through poststack impedance inversion and also generate one or more discontinuity attributes such as coherence and curvature.

A cursory examination of the 3D seismic volume (by way of vertical and horizontal sections) reveals bright amplitude anomalies in the shallow intervals, interspersed with many discontinuities interpreted as faults (Figure 2). Most of the bright amplitude anomalies appear to be coming from channels that show up well on the horizontal displays (time or horizon slices) as seen in Figure 3.

There may be several reasons for an amplitude anomaly to show up on seismic data. Besides seismic processing artefacts, a clean, high-porosity wet sand, tight sand, low-saturation gas sand, or a lateral change in lithology could exhibit a high amplitude anomaly. Similarly, streaks of salt, volcanics, or carbonates could indicate anomalies. Discriminating seismic anomalies associated with the presence of hydrocarbons from those that are not could be challenging. But it is important that such challenges are addressed so as to prevent costly drilling failures.

Impedance inversion

As our starting point, we decided to compute the coherence attribute so that it will provide a more accurate interpretation of the smaller as well as larger geologic features. We follow that up with model-based poststack impedance inversion to transform the seismic amplitude volume to into an impedance volume.

A segment of the inverted P-impedance section along a crossline passing through Atlantis well is shown in Figure 3. Notice, the high seismic amplitudes marked in green are associated with low impedance values. A stratal slice traversing one or more high amplitude anomalies is also shown in Figure 3, which is a composite visual display of impedance and coherence attributes. Some of the channel features show low impedance values in dark blue as indicated with light-blue arrows, and other channels show

high impedance fills as indicated with pale yellow arrows. Fault signatures are seen as black coherence lineaments.

The above workflow simply utilizes low impedance for screening out high seismic anomalies, and may not be sufficient for distinguishing bright amplitude anomalies associated with hydrocarbons from other geologic elements. For analyzing these, we turned to the well log data for Atlantis well where dipole sonic and density curves were available, and after computing different attributes such as Lambda-rho and Mu-rho (Goodway et al., 1997), we crossplotted them. On the Lambda-rho versus Mu-rho crossplot, we noticed that gas sand in the Snadd formation exhibited low values of Lambda-rho and high values of Mu-rho. Besides, there was an overlap between the points representing the gas sand and those coming from the Jurassic-Stø and Mid-Triassic Kobbe formations. But by bringing density into our analysis, it was possible to discriminate between them. Thus to extract Lambda-rho, Mu-rho and density volumes from seismic data, we decided to run prestack simultaneous impedance inversion, where multiple partial offset or angle substacks are inverted simultaneously. For each angle stack, a unique wavelet is estimated. Subsurface low-frequency models for P-impedance, S-impedance and density, constrained with appropriate horizons in the broad zone of interest, are constructed using the dipole sonic and density log data available for the Atlantis well.

Once the background models, wavelets and partial stacks were obtained, inversion analysis was carried out at the Apollo and Atlantis wells. After performing it at well locations, prestack simultaneous inversion was run for the full volume to extract P-impedance, S-impedance and density volumes. Even though it is an arduous task to extract density from seismic data due to unavailability of noise-free long offset data, we were able to extract it as the angle range for the available data extended to 47-48 degrees. Once we had the impedance volumes, Lambda-rho and Mu-rho attributes were generated and then we examined the anomalies in Lambda-rho – Mu-rho crossplot space.

We take this analysis forward through crossplotting the two attributes (Lambda-rho and Mu-rho), and picking up a cluster corresponding to low Lambda-rho and high Mu-rho enclosed in red polygon and shown in Figure 4a. On back-projecting these enclosed points on the vertical (Figure 4b) we see the variation in the two zones that we have considered prospective. This exercise on a line passing through Apollo well showed a similar response. We therefore conclude that all the high amplitude anomalies may not be associated with hydrocarbons, and we need to examine them with a different approach.

Next we crossplot density versus P-impedance as shown in Figure 5a for the line passing through the Atlantis well, and after enclosing the cluster points exhibiting low density and low impedance, and back-projecting, only the anomaly at the upper level is seen highlighted as shown in Figure 5b. We therefore conclude that we can trust this anomaly as being associated with hydrocarbons.

Thus by adopting a workflow that entails the generation of P-impedance, S-impedance and density attributes and examining these attributes first in the Lambda-rho versus Mu-rho crossplot space, and then in P-impedance versus Density crossplot space, it is possible to identify the fluid-associated anomalies.

Future directions

It is always instructive to carry out alternative workflows with different tools and compare the results for assessing the uncertainty in the exercise. Keeping in line with this strategy, we explore the application of spectral decomposition to the data at hand. In the context of DHIs, the basic premise is that reflections from fluid-saturated rocks are frequency-dependent. Goloshubin et al. (2006) found that reflection coefficient (water/gas) ratios are three times stronger at 14 Hz than at 50 Hz, and suggested that the observed reflection amplitudes be used for detecting liquid saturated areas in thin-porous layers. In the presence of hydrocarbons, the encasing formations selectively reflect some particular frequencies and not others, leading to high amplitudes on seismic sections. We used the matching pursuit method of spectral decomposition on the data at hand and noticed that many of the high amplitude anomalies are associated with higher spectral amplitudes, which are seen at 20 Hz or so (low frequencies) but not at higher frequencies, even though the bandwidth of the data extends to above 80 Hz. We do not claim that this analysis is conclusive, and more work will need to be done in this direction.

With regard to efforts being made in our industry for integration of seismic data with other types of data mitigating exploration risk, the patented P-cable multistreamer system holds promise. The controlled source electromagnetic (CSEM) method also serves as an independent source of information generating a volume of subsurface resistivity that can help locate pockets of hydrocarbon fluids. Multibeam seafloor mapping and sampling is also being done by some of the operators in that area. Plans are underway for integrating all this data for mitigating exploration risk.

Conclusions

We have addressed our objective of characterizing shallow bright amplitude anomalies with the application of prestack simultaneous impedance inversion and spectral decomposition. This has allowed us to discriminate between the bright amplitude anomalies that may be prospective from others that could be exhibiting high amplitudes due to other geologic conditions. The P-impedance, S-impedance and density attributes derived from simultaneous impedance inversion were crossplotted and zones exhibiting high seismic amplitudes were now examined in Lambda-rho versus Mu-rho crossplot space. Those high-amplitude seismic anomalies exhibiting low Lambda-rho and high Mu-rho, low-density and low P-impedance, as well as high

characteristic low-frequency signatures were considered prospective.

Acknowledgements

We wish to thank Arcis Seismic Solutions/TGS for encouraging this work and also for the permission to present and publish it.

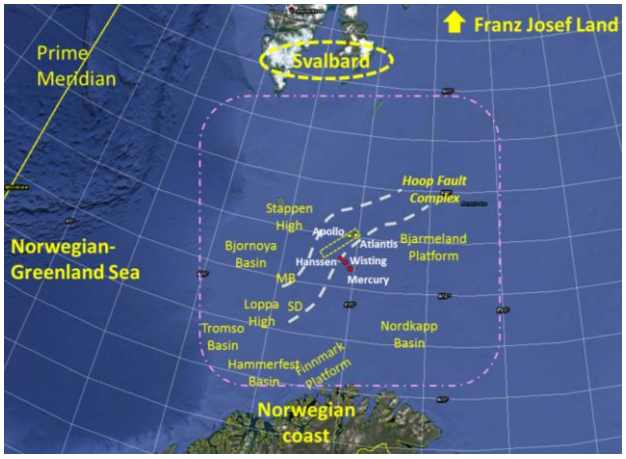

Figure 1: Location map showing the western Barents Sea. The corridor in white thick dashed lines shows the Hoop Fault system running roughly in a NE-SW direction. The location of the seismic data volume that was picked up for the present study is shown with the yellow dashed rectangle. *(Image generated using Google Earth)*

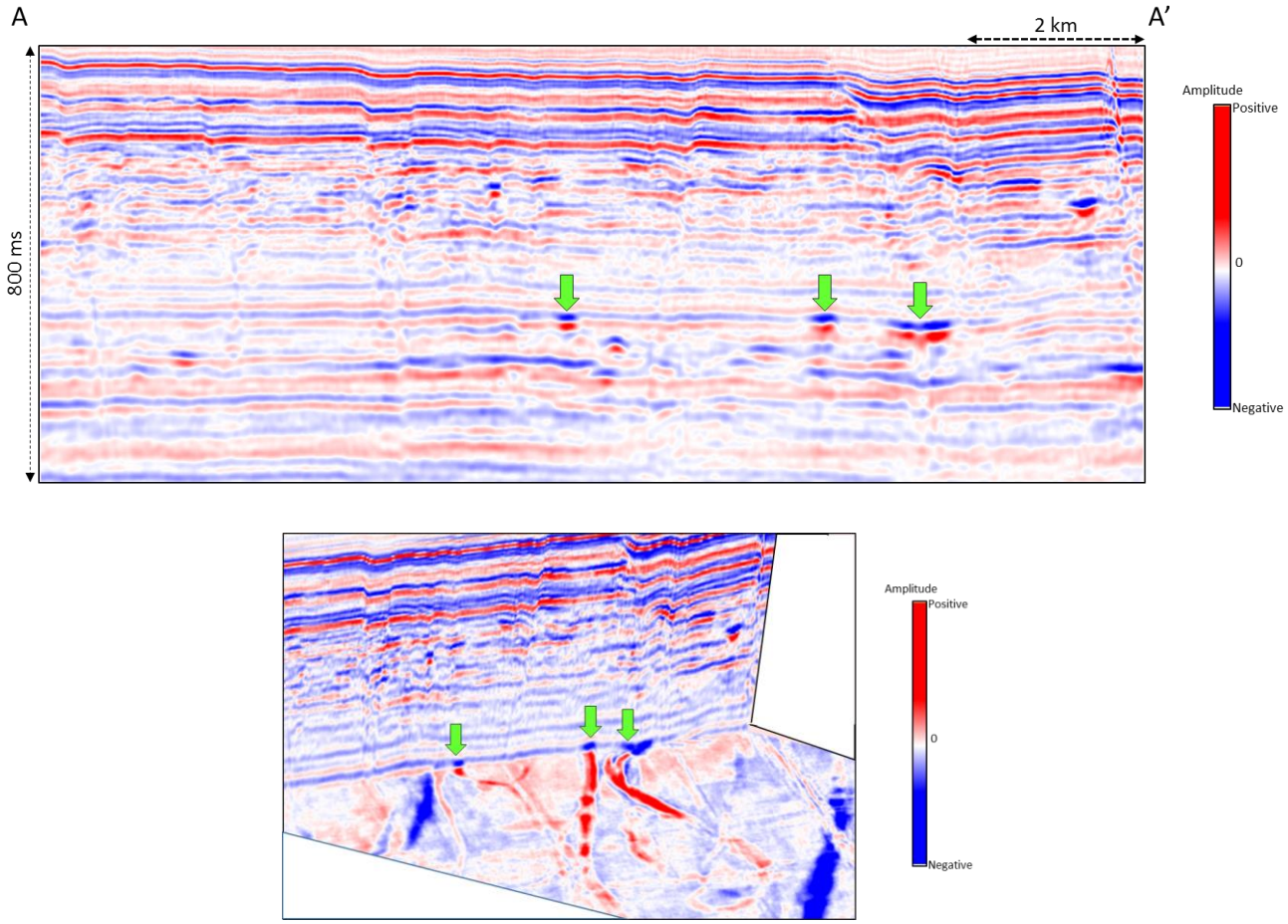

Figure 2 Inline AA' seismic section from the input seismic data. A number of bright spots are seen on the data. A chair display shows the amplitudes of the bright spots indicated with green arrows to be associated with subsurface channels. *(Data courtesy of TGS, Asker, Norway)*

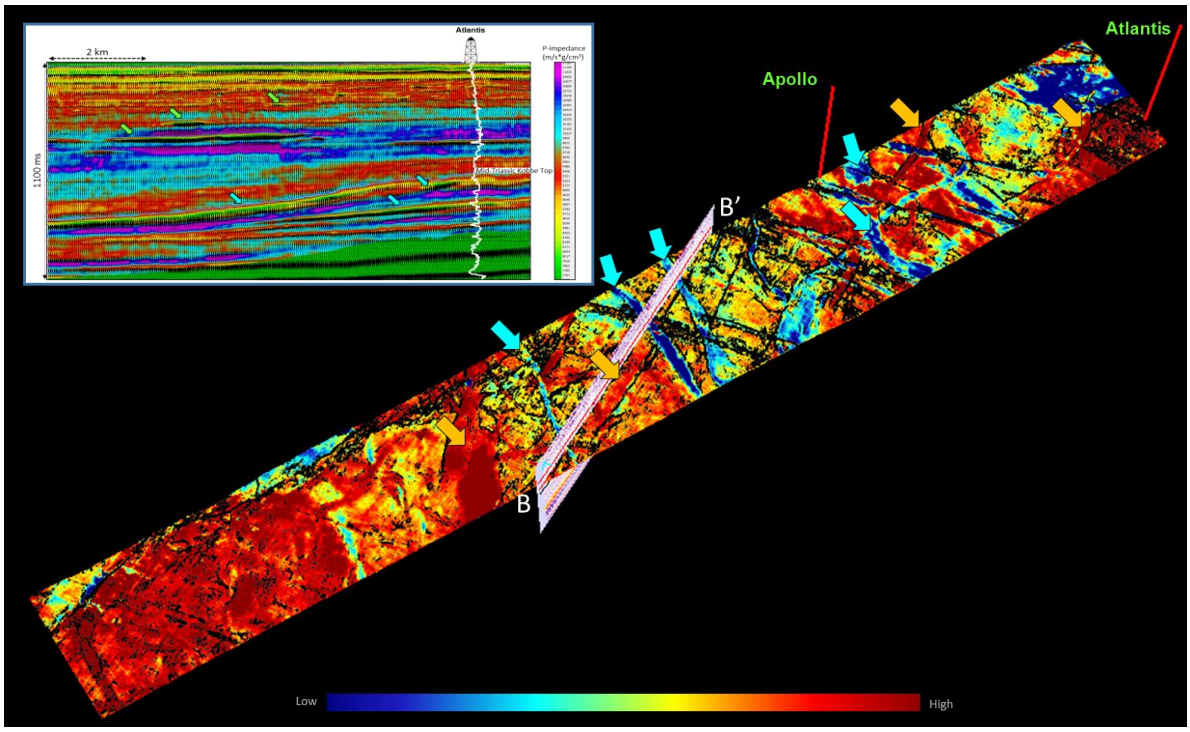

Figure 3: Stratal slice from the impedance volume with overlay of energy-ratio coherence. Notice low impedance in blue seen in the channels indicated with cyan arrows and high impedance indicated with pale yellow arrows. Inverted P-impedance section with seismic overlay along a crossline passing through well Atlantis. The log curve overlaid in white is the computed P-impedance. The high seismic amplitudes marked in green are seen to be associated with lower impedance values. *(Data courtesy of TGS, Asker, Norway)*

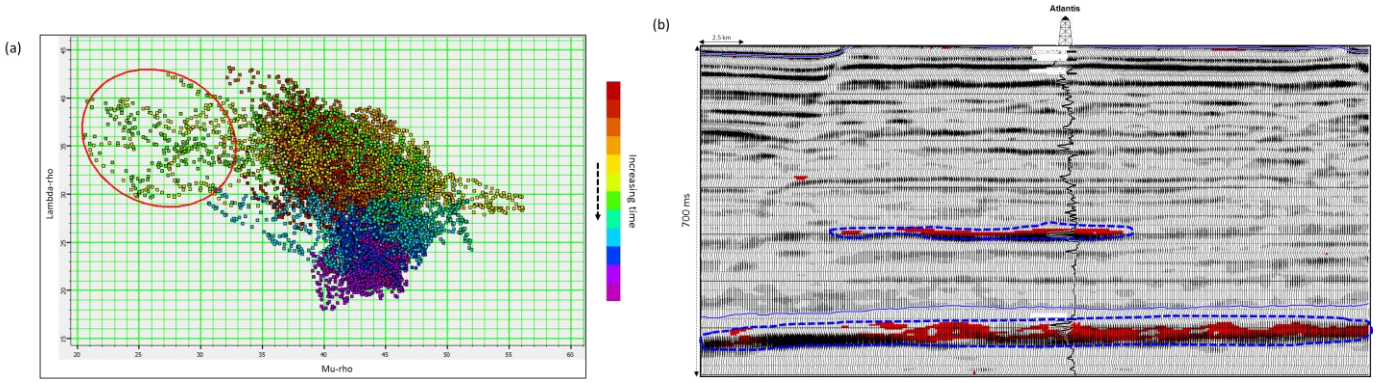

Figure 4: (a) Crossplot between Lambda-rho and Mu-rho attributes from the impedance section shown in Figure 3 passing through the Atlantis well. The points in the red polygon represent low values of Lambda-rho and high values of Mu-rho, which could be considered as representing prospective sandstones probably impregnated with gas. On back-projecting them on to the vertical section as shown in (b), we notice they are coming from two different levels. *(Data courtesy of TGS, Asker, Norway)*

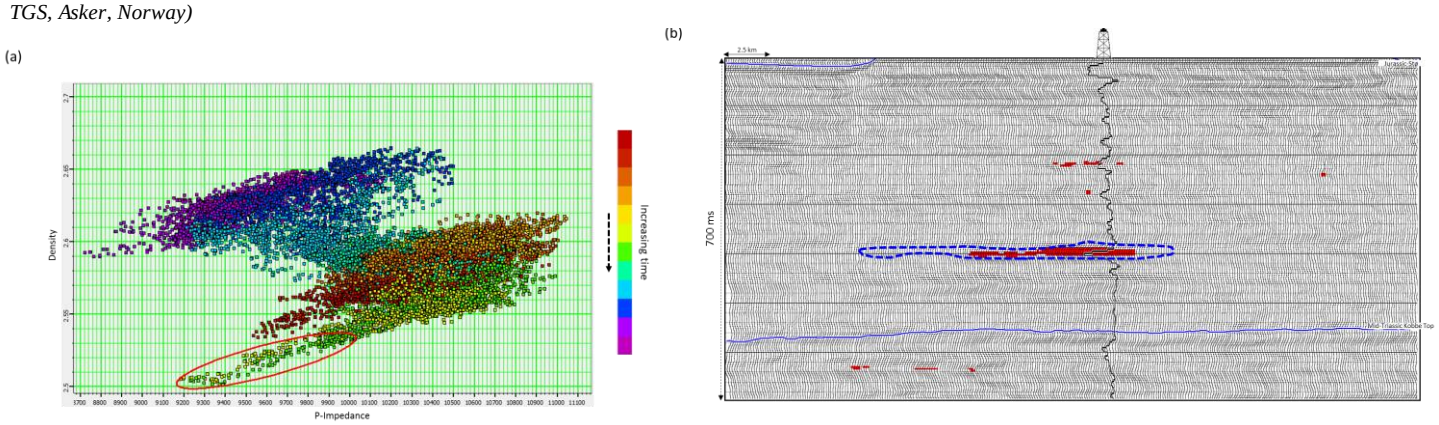

Figure 5: Crossplot between P-impedance and density attributes derived from simultaneous inversion. Back-projecting the points in the red polygon on to the vertical section shows that they highlight only the anomaly at the upper level, and not the lower one.

EDITED REFERENCES

Note: This reference list is a copyedited version of the reference list submitted by the author. Reference lists for the 2017 SEG Technical Program Expanded Abstracts have been copyedited so that references provided with the online metadata for each paper will achieve a high degree of linking to cited sources that appear on the Web.

REFERENCES

Bünz, S., A. Plaza-Faverola, S. Hurter, and J. Mienert, 2014, 4D seismic study of active gas seepage systems on the Vestnesa Ridge, offshore W-Svalbard, EGU General Assembly Conference Abstracts, 16026.

Goloshubin, G., C. Van Schuyver, V. Korneev, D. Silin, and V. Vingalov, 2006, Reservoir imaging using low frequencies of seismic reflections: The Leading Edge, 25, 527–531, http://dx.doi.org/10.1190/1.2202652.

Goodway, B., T. Chen and J. Downton, 1997, Improved AVO fluid detection and lithology discrimination using Lame petrophysical parameters; 'λρ, 'μρ', & 'λ/μ' fluid stack' from P and S inversions: 67th Annual International Meeting, SEG, Expanded Abstracts, 183–186, https://doi.org/10.1190/1.1885795.